TECHNICAL REPORT NO. 15

TO

The Office of Naval Research
Contract No. N00014-86-K-0381

CYCLIC STRESS-STRAIN BEHAVIOR OF TITANIUM IN THE PRESENCE OF POROSITY

D. A. Gerard+ D. A. Koss

Department of Materials Science and Engineering
The Pennsylvania State University
University Park, PA 16802

+Currently: General Motors Technical Center
Warren, MI 48090

SECURITY CLASSIFICATION OF THIS PAGE

REPORT DOCUMENTATION PAGE

Form Approved
OMB No. 0704-0188

1a REPORT SECURITY CLASSIFICATION	1b RESTRICTIVE MARKINGS
2a SECURITY CLASSIFICATION AUTHORITY	3 DISTRIBUTION / AVAILABILITY OF REPORT
2b DECLASSIFICATION / DOWNGRADING SCHEDULE	
4 PERFORMING ORGANIZATION REPORT NUMBER(S) Report No. 15	5 MONITORING ORGANIZATION REPORT NUMBER(S)
6a NAME OF PERFORMING ORGANIZATION The Pennsylvania State Univ.	6b OFFICE SYMBOL (If applicable) / 7a NAME OF MONITORING ORGANIZATION
6c. ADDRESS (City, State, and ZIP Code) Dept. of Materials Science & Engineering The Pennsylvania State University University Park, PA 16802	7b ADDRESS (City, State, and ZIP Code)
8a. NAME OF FUNDING / SPONSORING ORGANIZATION Office of Naval Research	8b OFFICE SYMBOL (If applicable) / 9 PROCUREMENT INSTRUMENT IDENTIFICATION NUMBER
8c. ADDRESS (City, State, and ZIP Code) Office of Naval Research, Code 1131 800 N. Quincy Street Arlington, VA 22217	10 SOURCE OF FUNDING NUMBERS PROGRAM ELEMENT NO / PROJECT NO / TASK NO / WORK UNIT ACCESSION NO

11 TITLE (Include Security Classification)
Cyclic Stress-Strain Behavior of Titanium in the Presence of Porosity

12. PERSONAL AUTHOR(S)
D A. Gerard and D. A. Koss

13a TYPE OF REPORT	13b TIME COVERED FROM _____ TO _____	14 DATE OF REPORT (Year, Month, Day)	15 PAGE COUNT
		April 1989	11

16 SUPPLEMENTARY NOTATION

17 COSATI CODES			18 SUBJECT TERMS (Continue on reverse if necessary and identify by block number)
FIELD	GROUP	SUB-GROUP	
			Porosity, Casting, Low Cycle Fatigue, Cyclic Stress-Strain, Powder processed titanium,

19 ABSTRACT (Continue on reverse if necessary and identify by block number)

The cyclic stress-strain behavior of powder-processed titanium containing 0.4 to 6.0 volume percent rounded porosity has been examined at room temperature. Total strain-range testing at small amplitudes such as 0.375% indicates that porosity has little influence on the cyclic hardening/softening response. However, at large total strain ranges such as 1.5%, the cyclic flow behavior of the porous materials differs from that of fully dense titanium, behaving similarly to the pore-free material cycled at significantly higher strain amplitudes. The differences in cyclic flow behavior are believed to be a result of the locally large strain amplitudes induced adjacent to the pores. Determinations of the cyclic strain-hardening exponents indicate no significant effect of porosity with n-values ranging from 0.24 to 0.28 for all of the materials examined.

20 DISTRIBUTION / AVAILABILITY OF ABSTRACT	21 ABSTRACT SECURITY CLASSIFICATION
☐ UNCLASSIFIED/UNLIMITED ☒ SAME AS RPT ☐ DTIC USERS	UNCLASSIFIED
22a NAME OF RESPONSIBLE INDIVIDUAL Doanald A. Koss	22b TELEPHONE (Include Area Code) 814-865-5447 / 22c OFFICE SYMBOL

DD Form 1473, JUN 86 — Previous editions are obsolete — SECURITY CLASSIFICATION OF THIS PAGE

S/N 0102-LF-014-6603

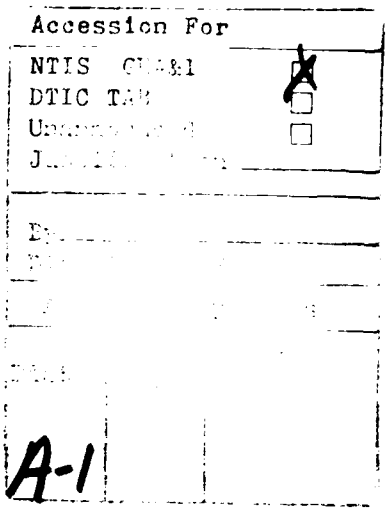

CYCLIC STRESS-STRAIN BEHAVIOR OF TITANIUM IN THE PRESENCE OF POROSITY

D. A. Gerard* and D. A. Koss

Department of Materials Science and Engineering
The Pennsylvania State University
University Park, PA 16802

*Currently: General Motors Technical Center
Warren, MI 48090-9040

ABSTRACT

The cyclic stress-strain behavior of powder-processed titanium containing 0.4 to 6.0 volume percent rounded porosity has been examined at room temperature. Total strain-range testing at small amplitudes such as 0.375% indicates that porosity has little influence on the cyclic hardening/softening response. However, at large total strain ranges such as 1.5%, the cyclic flow behavior of the porous materials differs from that of fully dense titanium, behaving similarly to the pore-free material cycled at significantly higher strain amplitudes. The differences in cyclic flow behavior are believed to be a result of the locally large strain amplitudes induced adjacent to the pores. Determinations of the cyclic strain-hardening exponents indicate no significant effect of porosity with n-values ranging from 0.24 to 0.28 for all of the materials examined.

INTRODUCTION

Powder-processed and cast materials are often not utilized in fatigue limiting applications due to inherent processing defects such as porosity. Many investigations have examined the deleterious effects of porosity on high cycle fatigue; for examples see Refs. [4-12]. The reductions in high cycle fatigue life of porous materials are generally attributed to local stress concentrations adjacent to pores that generate localized slip in the nominally elastic matrix. More recently the present investigators have shown that a similar phenomena occurs during low cycle fatigue (LCF) deformation in the presence of porosity[1,2].

The purpose of this investigation is to examine the cyclic flow behavior of porous titanium, and to analyze the results in terms of the properties which have been obtained for fully dense titanium in the present, as well as, other investigations[13,14]. In order to verify the enhanced plastic flow adjacent to pores two strain amplitudes are examined and the results are analyzed from both microscopic and macroscopic perspectives. The overall influence of porosity on LCF is to be discussed in a future

publication[15], while the effects of porosity on crack initiation short crack growth during LCF are described elsewhere[1-3].

EXPERIMENTAL PROCEDURE

Conventional powder metallurgy processing techniques utilizing the sequential processes of cold isostatic pressing, sintering, swaging, and resintering were used to prepare low cycle fatigue specimens of commercially pure titanium. The processing histories of the materials as a function of pore content are described elsewhere[16]. Commercially pure wrought titanium having essentially the same impurity content as the powder-processed specimens was used for comparing the fatigue properties of the fully dense and porous materials. In each of the cases, the materials contained between 0.13 and 0.15 wt.% oxygen.

The fully dense and porous microstructures containing 0.4%, 1.5% and 6% isolated porosity as well as 6% interconnected porosity are shown in Fig 1. Stereopycnometer results confirmed that the pores were isolated in all but the interconnected condition; see Fig. 1e. The microstructures in the isolated porosity specimens consist of well-rounded elliptical pores which have an average radius* of 10 to 15 microns and an average aspect ratio (major to minor diameter) of 1.3. Fig. 1e shows that when the interconnected-porosity specimens are examined in cross section, the pores have an average radius of about 25 microns, and have an average aspect ratio of approximately 1.9. It should also be noted that the grain sizes were of the same magnitude in size for the fully dense, 1.5% and 6% porous materials (~40 μm grain size), but a grain size of 140 μm was obtained in the 0.4% material.

Fully reversible low cycle fatigue tests were performed at room temperature in total strain control at ranges of 0.75 and 1.5%. The lower strain-range tests were conducted at a frequency of 0.25 Hz while the larger strain-amplitude tests were performed at 0.15 Hz, both with a triangular waveform. Cylindrical push-pull low cycle fatigue specimens were used for this investigation; the specimens had a gage length of 15 mm and a 6.4 mm diameter. Prior to testing the specimens surfaces were polished, and then subsequently vacuum annealed at 700°C for 0.5 hours at a pressure of 3×10^{-3} Pa.

EXPERIMENTAL RESULTS AND DISCUSSION

In order to analyze the influence of porosity on low cycle fatigue, the influence of porosity on the cyclic flow properties of titanium must be understood. In Fig. 2, the cyclic flow behavior, as described by the average peak stress, is shown for fully dense and porous titanium. At the lower strain range, 0.75%, the fully dense and porous specimens are essentially cyclically stable for approximately the first 100 cycles after which cyclic softening begins to occur; see Fig. 2a.

The cyclic flow behavior at 1.5% total strain range is markedly different for the fully dense and porous materials. The fully dense material behaves in a similar manner as it did at the lower strain amplitude, being cyclically stable for approximately 100 cycles followed by cyclically softening. In contrast, the results presented in Fig. 2b indicate that the porous materials initially harden for the first few hundred cycles after which cyclic softening occurs.

---

* The average radius is the average value of the Martin radii. For this study the Martin radii are defined as the distance from the center of gravity of the pore to its edge; the initial radius measurement is taken at an arbitrary angle of 0° after which the remaining seven radii are obtained at angles of 45° to 315° in 45° increments.

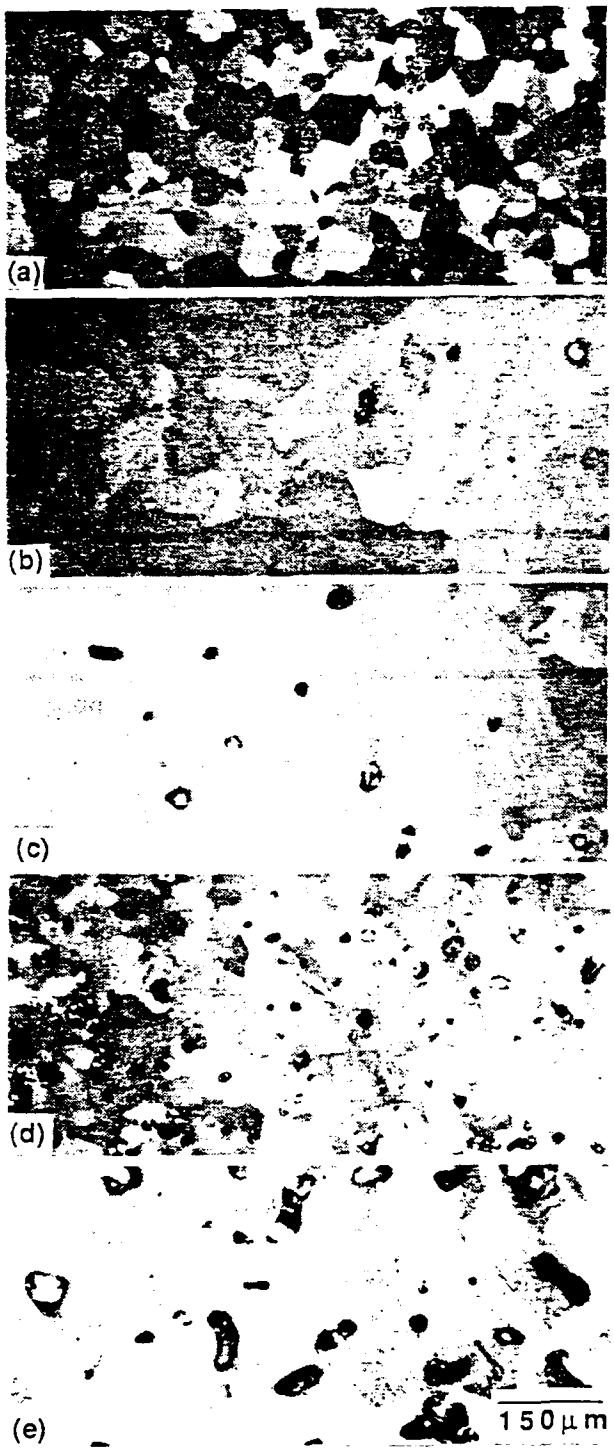

Figure 1. Polarized light micrographs of titanium containing (a) 0% porosity, (b) 0.4% isolated porosity, (c) 1.5% isolated Porosity, (d) 6% isolated porosity, and (e) 6% interconnected porosity. The bright reflections are from the epoxy used to preserve the original pore shape during polishing. All micrographs have the same magnification.

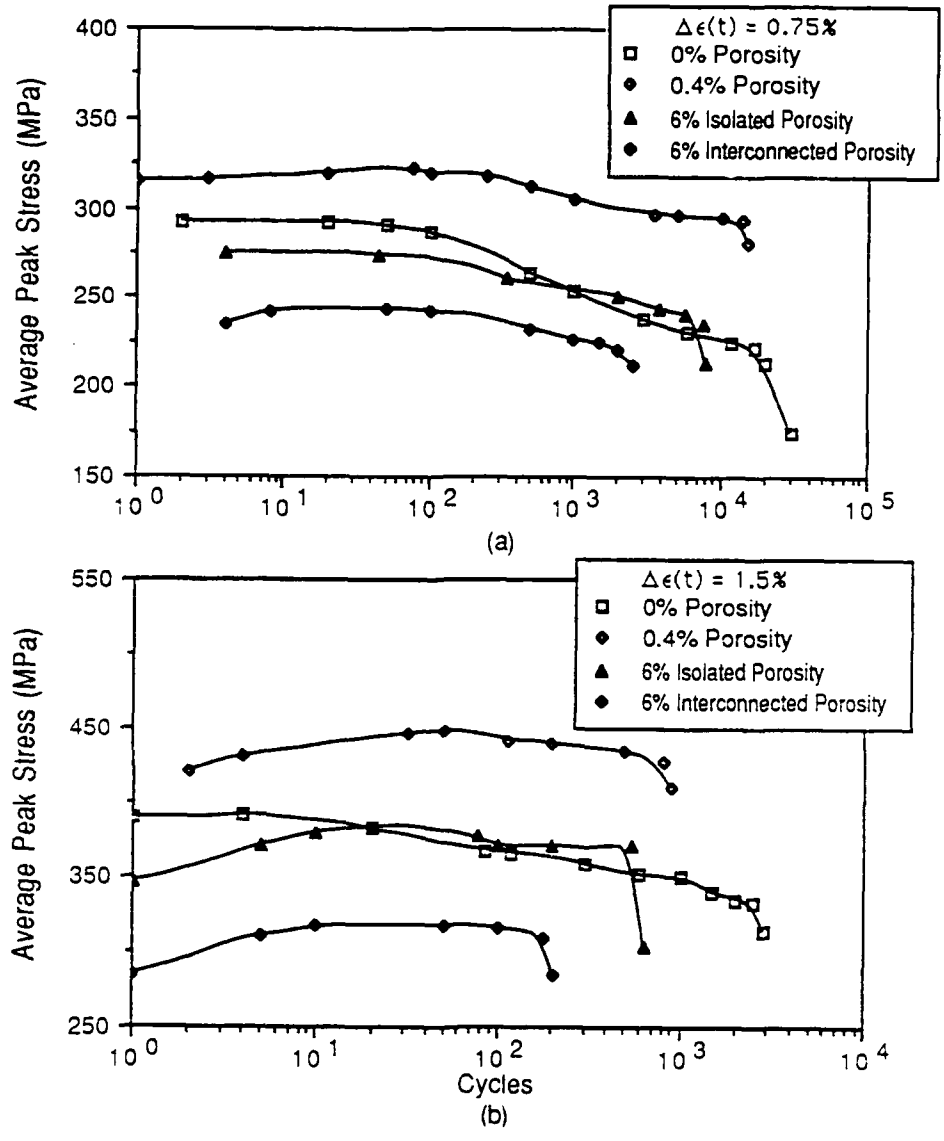

Figure 2. The cyclic stability of the fully dense and porous titanium material subjected to total strain range testing of (a) 0.75%, and (b) 1.5%.

The cyclic deformation results from this study agree with the observations of Stevenson and Breedis[13] and Plumtree et. al.[14] for the cyclic deformation of fully dense titanium which had similar compositions and grain sizes to those in this investigation. The results from the Stevenson and Breedis[13] investigation indicate that for plastic strain amplitudes greater than ±1.0% titanium cyclically hardens from the onset of testing to failure. In contrast, at plastic strain amplitudes between ±0.3% and ±1.0% titanium exhibits a cyclic hardening response followed by cyclic softening. The amount of cyclic hardening is reduced with decreasing strain amplitude while the degree of softening increases; this is consistent with the data in Fig. 2.

Stevenson and Breedis[13] (S&B) as well as other investigators[17-20] have used transmission electron microscopy in attempting to explain the cyclic hardening behavior of titanium. S&B concluded that the cyclic hardening which occurs in titanium results from bulk deformation behavior being dominated by segments of long screw dislocations which extend across relatively dislocation-free regions and terminate at each end within a dislocation cell wall substructure. It was hypothesized that the screw dislocations are segments of mixed dislocations which have been left behind by faster moving edge dislocations. Upon further cycling the screw dislocations form jogs/dipoles which not only act as barriers to the screw dislocation motion (which results in cyclic hardening) but also act as sources for the generation of edge dislocations. The jogs have been shown in another investigation[21] to act as barriers for screw dislocation motion, but not for edge dislocation motion. Upon further cycling, the edge dislocation density is believed to become high enough to control the overall bulk deformation behavior, and as a result the higher velocity edge dislocations promote cyclic softening. Thus, cyclic softening should commence when the edge dislocation density begins to dominate the bulk flow behavior.

The cyclic flow behavior trends observed in Fig. 2 can be explained in terms of the above results and the hypothesis offered by S&B[13]. The fully dense materials show cyclic stability initially at both strain amplitudes followed by cyclic softening. This result is not surprising for either the 0.75% or 1.5% total strain range tests since the plastic strain amplitudes under these conditions are approximately ±0.1% and ±0.375%, respectively. Recall that S&B[13] observed no cyclic hardening at plastic strain amplitudes below ±0.3% and very minimal hardening at plastic strain amplitudes at levels just above the same plastic range.

The cyclic flow behavior of the porous materials may be understood in the following manner. At low strain amplitudes, the porous materials behave in a similar manner to the fully dense material, first exhibiting cyclical stability followed by cyclic softening (see Fig. 2a). However, as previously described, at the higher strain amplitude the porous materials first cyclically harden and then soften, behaving as the fully dense material cyclically deformed at the intermediate plastic strain amplitudes (0.3 to 1.0%) in the S&B study[13]. Comparisons of the results in Fig. 2 with fully dense titanium tested over a broad range of strain amplitudes[13,14] indicate that the porous materials exhibit a cyclic hardening response similar to that of the fully dense materials being cycled at approximately double the plastic strain amplitude.

The above influence of porosity on the cyclic flow behavior is likely due to a combination of factors. The most dominant factor may be attributed to pore-induced stress and strain concentrations adjacent to the pores. These plastic zones result in an effectively higher strain amplitude in the region surrounding pores. As a result, a significant volume of the porous specimens experience locally high strain amplitudes. The volume of material affected by the pore-induced strain concentrations scales with the pore's size and imposed macroscopic strain amplitude. A schematic profile of the enhanced strain amplitude which is generated adjacent to a pore at the maximum tensile stress on the plane of maximum stress concentration for a given cycle is shown in Fig. 3. Refs.(1,2) contain experimental strain data adjacent to a hole which verify this profile. At the higher cyclic strain amplitude, a volume of material within a distance of about 1.5 pore diameters adjacent to pores would be expected to deform at

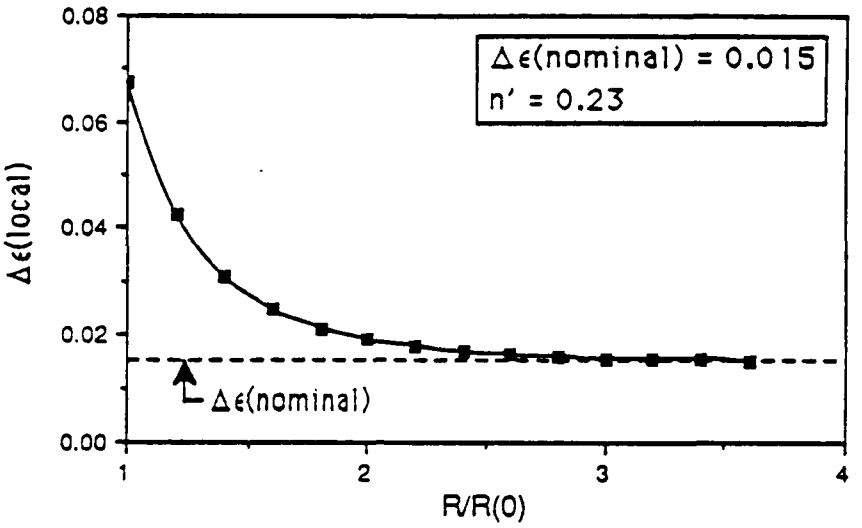

Figure 3. The theoretical profile of a local strain distribution, distribution adjacent to an elliptical pore in a plastically deforming matrix. The profile has been estimated at the peak tensile load of a cycle on the plane of maximum strain concentration over a normalized distance R/R(0).

plastic strain amplitudes significantly above ±0.3% (this is not the case for the porous materials tested at the lower strain amplitude). Although it is not intuitively apparent, three-dimensional calculations assuming a spherical pore shape indicate that approximately 11% of the volume of the 0.4% porous material is influenced by the porous regions (i.e., ~1.5 times the pore diameter) and therefore is being subjected to the higher strain gradients. As a result, the macroscopic flow behavior is significantly influenced by the stress concentration effects of pores even at low porosity levels (0.4%). In view of the above, it is not surprising that each of the porous titanium conditions examined at the total strain amplitude of 1.5% cyclically behave by initially hardening and subsequently softening similar to fully dense material being deformed at higher strain amplitudes.

Another method of examining the stability of material subjected to cyclic straining is to monitor the total plastic strain developed throughout a cycle as a function of fatigue life. When a material cyclically hardens during total strain amplitude testing, the plastic strain amplitude of the material will decrease as the material becomes more resistant to plastic flow, with the converse being true for cyclic softening. An examination of the plastic strain amplitude behavior indicated behavior which correlates fairly well with that observed when monitoring the cyclic peak stresses is shown in Fig. 2. At 0.75% total strain range, the plastic strain amplitude tends to increase at least slightly during fatigue life, which agrees with the general cyclic softening behavior trends presented in Fig. 2a. During the high strain amplitude fatigue (i.e., 1.5% total strain range control), the fully dense titanium shows an increase in the plastic strain range during testing while each of the porous materials showed a reduction in the plastic strain range. The increase in the plastic strain range observed for the fully dense material is in agreement with the cyclic softening behavior which was observed, as does the decrease in plastic strain range with the initial cyclic hardening behavior which occurs in the porous materials.

An interesting observation is that the magnitude of the plastic strain amplitudes are especially large in the 6% interconnected-porosity material. This is not surprising in view of the significantly lower peak stresses measured and presented in Fig. 2. The lower peak stress of the 6% interconnected-porosity titanium may be attributed to the lower yield stress in the material; note, the tensile properties of these materials are discussed elsewhere[16]. The lower yield stress and thus resulting cyclic flow stress for this material, even when compared with the 6% isolated-porosity titanium, may be partially accounted for by the significantly higher elliptical pore aspect ratio of the interconnected material (1.3 vs. 1.9). The larger stress concentrations associated with the sharper pores in the 6% interconnected porous material should reduce the proportional limit of the material, and thereby should be partially accountable for the reduction in the cyclic peak stresses.

The cyclic work-hardening exponent n is frequently used to analyze low cycle fatigue. In this study the cyclic work-hardening exponent is estimated with the increasing loading portion of the hysteresis loop as was first purposed by Morrow[22]. Although this is not a rigorous technique for obtaining the cyclic work-hardening exponent, the methodology has been shown to be accurate in approximating the cyclic work-hardening exponent for metals when the plastic and elastic strains generated at the peak strain are approximately equal, which is the case in this study.[22] More specifically, Morrow has shown that when the elastic and plastic strains for a hysteresis are roughly equal, the increasing stress side of the hysteresis loop frequently resembles the cyclic stress-strain curve obtained from the conventional stable hysteresis data. Thus a reasonable estimation of the cyclic work-hardening exponent should obtainable in this study. There are numerous methods for obtaining the cyclic stress-strain curve which are described in detail elsewhere[23,24], and therefore are not be discussed here.

Fig. 4 shows the variation of the cyclic work-hardening exponent as a function of fatigue life for the porous and fully dense materials. It is recognized that the cyclic work-hardening exponent is generally obtained after cyclic stability has

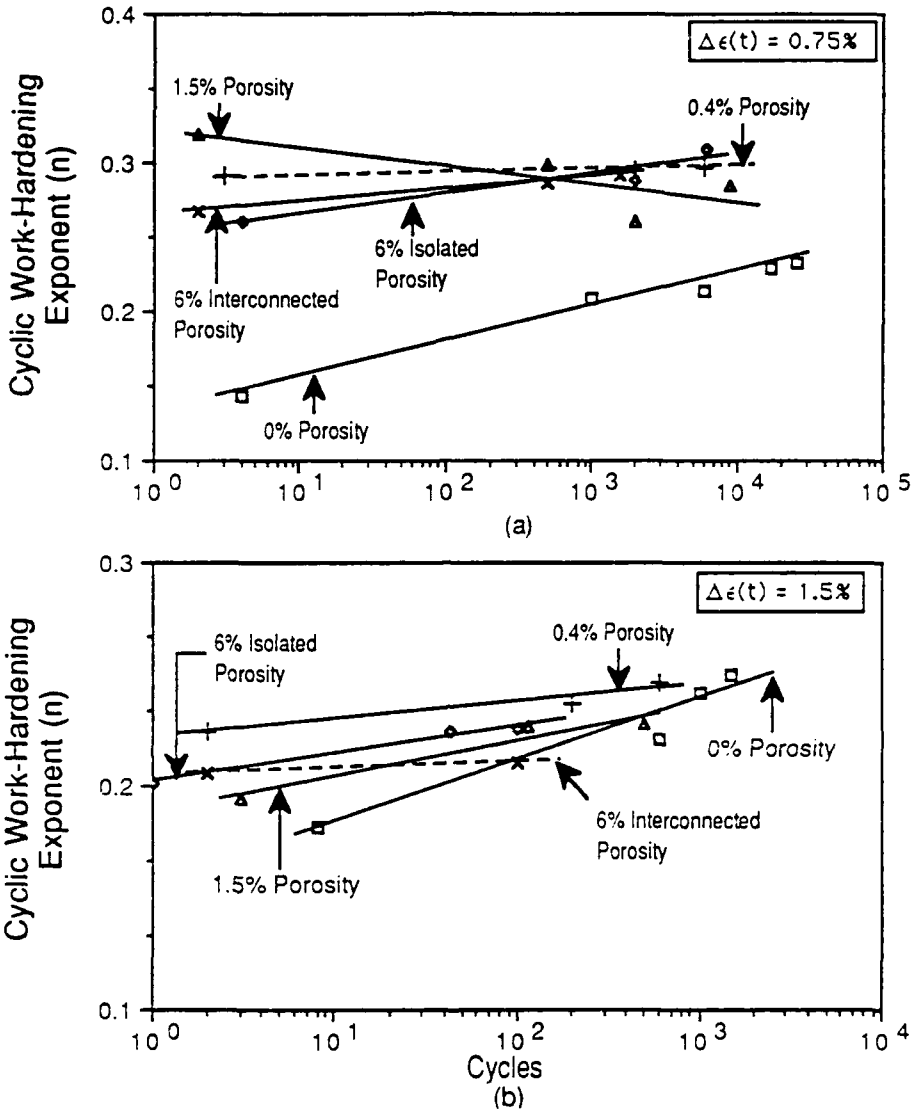

Figure 4. The variation in the cyclic work-hardening exponent for the fully dense and porous titanium materials during total strain range testing at (a) 0.75%, and (b) 1.5%.

been achieved. However, since cyclic stability for the porous materials does not readily occur (see Fig. 2) the results are presented as a function of the number of cycles.

Fig. 4a indicates that the n-values of the porous materials tend to converge to a value around 0.28 at the 0.75% total strain range and 0.24 to 0.26 at the 1.5% strain range. These n-values are similar to those of Puskár[25] (0.275) and to results from this study (0.285) which have been obtained for the fully dense titanium utilizing more rigorous testing techniques for determining the cyclic work-hardening exponent that were eluded to above. The more comprehensive evaluation for the cyclic work-hardening exponent has been obtained from the testing of several specimens throughout a broad range of plastic strain amplitudes (±0.1% to ±1.4%); the plastic strain amplitudes and peak stress amplitudes were analyzed at half of the total fatigue life for each of the strain amplitudes examined.

In Fig. 4b it is shown that when testing at 1.5% total strain range, the fully dense titanium and the isolated porosity materials all display an increase in the cyclically work-hardening exponent throughout the fatigue life. As in the case of the lower strain amplitude, the cyclic work-hardening values roughly converge at a value of 0.25. Thus the n-value obtained during the high strain amplitude tests is somewhat lower than that obtained at the lower strain amplitude (0.28) or that measured by a multiple-specimen strain amplitude technique (0.285). Although the limitations of the single hysteresis loop for determining the n-value are described above, there is little doubt that part of the difference in the n-values using the two techniques is associated with the well known inadequacy of the $\sigma = k\varepsilon^n$ equation in predicting the stress-strain response at low strains. Nonetheless, the above results for the cyclic work-hardening exponent support the relationship developed by Morrow[22] for approximating the conventional cyclic strain-hardening exponent from the loading side of the hysteresis loop; see Ref (16).

CONCLUSIONS

Porosity can significantly influence the cyclic flow behavior under low cycle fatigue conditions. Little difference is observed in the cyclic hardening/softening behavior of the fully dense and porous titanium at 0.75% total strain range testing. However, for 1.5% total strain range tests, significant changes in the cyclic flow behavior are observed between the porous and fully dense materials. Examination of the local strain profiles near the pores indicate that the differences in the cyclic flow behavior appear to be a result of the locally large strain amplitudes which are generated adjacent to the pores. Even at low levels of porosity (0.4%) the material cyclically behaves (i.e., hardening/softening behavior) as if it were being subjected to significantly higher strain amplitudes when compared with the fully dense material.

The cyclic work-hardening exponent was determined as a function of cycles utilizing Morrow's[22] hysteresis technique to estimate the cyclic stress-strain response. Even though cyclic stability was generally not obtained for the various material conditions, the values at which the data for both the porous and fully dense materials converged are in fairly good agreement with more rigorous cyclic work-hardening exponent results obtained from conventional cyclic stress-strain analyses.

ACKNOWLEDGEMENTS

This work has been graciously supported by the Office of Naval Research through Contract No. N00014-86-K-0381.

REFERENCES

1. D. A. Gerard and D. A. Koss, "Porosity and Crack Initiation During Low Cycle Fatigue", submitted to and accepted for publication by Material Science and Engineering A (1990).

2. D. A. Gerard and D. A. Koss, "A Model for the Effect of Porosity on Crack Initiation During Low Cycle Fatigue", submitted for publication.

3. D. A. Gerard and D. A. Koss, "The Influence of Porosity on Short Fatigue Crack Growth at Large Strain Amplitudes", submitted for publication.

4. R. Haynes, Powder Metal., 1, pp. 17-20 (1977).

5. R. S. Bankowski and W. H. Feilbach. Int. J. of Powder Metall., 6 (3), pp. 23-37 (1970).

6. D. Eylon, Y. Mahajan, N. R. Ontko and F. H. Froes, Proc. AIME Symp. on Titanium Powder Metallurgy (1980).

7. P. R. Smith, D. Eylon, S. W. Schwenker and F. H. Froes, Advanced Processing Methods for Titanium, Eds. D. F. Hasson and C. H. Hamilton, From TMS of AIME held in Louisville, KY, pp. 61-77 (1981).

8. P. DiMascio and R. A. Queeney, Int. J. of Powder Metall. & Powder Tech., 19 (2), pp. 127-135 (1983).

9. J. Konda and K. Okita, Powder Metall. 18, p. 302 (1972).

10. N. E. Frost, K.J. Marsh, and L. P. Pook, Metal Fatigue, Clarendon Press, Oxford (1974).

11. F. Soniak and L. Remy, The Behavior of Short Fatigue Cracks, EFG Pub. 1, Eds. K.J. Miller and E.R. de los Rios, Mechanical Engineering Publications, London, pp. 133-142 (1986).

12. A. Fathulla, B. Weiss and R. Stickler, The Behavior of Short Fatigue Cracks, EFG Pub. 1, Eds. K.J. Miller and E.R. de los Rios, Mechanical Engineering Publications, London, pp. 115-132(1986).

13. R. Stevenson and J. F. Breedis, Acta Metallurgica, 23, pp. 1419-1429 (1975).

14. J. I. Dickson, J. Ducher and A. Plumtree, Metallurgical Transactions A, 7A, pp. 1559-1565 (1976).

15. D. A. Gerard and D. A. Koss, unpublished research (1989).

16. D. A. Gerard, Ph.D. Dissertation, Michigan Technological University (1989).

17. D. Munz, Eng. Fracture Mechanics, 5, pp. 353-364 (1973).

18. D. Munz, Scripta Metallurgica, 6, pp. 815-820 (1972).

19. J. I. Dickson, L. Handfield and G. L'Esperance, Materials Science and Engineering, 60, pp. L3-L7 (1983).

20. L. Handfield and J. I. Dickson, Defects, Fracture and Fatigue, Eds., G. C. Sih and J. W. Provan, Proceedings of 2nd Int. Symposium - Mont Gabriel, Canada, May 30-June 5, 1982, pp 37-51 (1983).

21. M. Klesnil and P. Lukasm J. Iron Steel Inst, 205, p. 746 (1967).

22. J-D. Morrow, Internal Friction, Damping and Cyclic Plasticity, ASTM STP 378, American Society for Testing Materials, Philadelphia, PA, pp. 45-87 (1965).

23. R. W. Landgraf, J-D. Morrow and T. Endo, J. of Materials, 4 (1), pp. 176-188 (1969).

24. R. W. Landgraf, Achievement of High Fatigue Resistance in Metals and Alloys, ASTM STP 467, Am. Soc. for Testing and Materials, pp. 3-36 (1970).

25. A. Puskár, Materials Science and Engineering, 61, pp. 111-116 (1983).